General Disclaimer

One or more of the Following Statements may affect this Document

- This document has been reproduced from the best copy furnished by the organizational source. It is being released in the interest of making available as much information as possible.

- This document may contain data, which exceeds the sheet parameters. It was furnished in this condition by the organizational source and is the best copy available.

- This document may contain tone-on-tone or color graphs, charts and/or pictures, which have been reproduced in black and white.

- This document is paginated as submitted by the original source.

- Portions of this document are not fully legible due to the historical nature of some of the material. However, it is the best reproduction available from the original submission.

AIRFOIL SECTION DRAG REDUCTION AT TRANSONIC SPEEDS

BY NUMERICAL OPTIMIZATION

Raymond M. Hicks, Garret N. Vanderplaats

Ames Research Center
Moffett Field, Calif. 94035

Earll M. Murman

Flow Research, Inc.
Kent, Washington

and

Rosa R. King

Computer Sciences Corp.
Mountain View, California

1. Report No. TM X-73,097	2. Government Accession No.	3. Recipient's Catalog No.
4. Title and Subtitle AIRFOIL SECTION DRAG REDUCTION AT TRANSONIC SPEEDS BY NUMERICAL OPTIMIZATION		5. Report Date
		6. Performing Organization Code
7. Author(s) Raymond M. Hicks, Garret N. Vanderplaats, Earll M. Murman,* and Rosa R. King†		8. Performing Organization Report No. A-6407
9. Performing Organization Name and Address Ames Research Center, Moffett Field, Calif. 94035 *Flow Research, Inc., Kent, Washington †Computer Sciences Corp., Mountain View, Calif.		10. Work Unit No. 505-06-31
		11. Contract or Grant No.
		13. Type of Report and Period Covered Technical Memorandum
12. Sponsoring Agency Name and Address National Aeronautics and Space Administration Washington, D. C. 20546		14. Sponsoring Agency Code
15. Supplementary Notes		

16. Abstract

A practical procedure for the design of low drag, transonic airfoils is demonstrated. The procedure uses an optimization program, based on a gradient algorithm coupled with an aerodynamic analysis program, that solves the full, non-linear potential equation for transonic flow. The procedure is useful for the design of retrofit modifications for drag reduction of existing aircraft as well as for the design of low drag profiles for new aircraft. Results are presented for the modification of four different airfoils to decrease the drag at a given transonic Mach number.

17. Key Words (Suggested by Author(s)) Aerodynamics Airfoil Wing Airplane design Computer design		18. Distribution Statement Unlimited STAR Category - 02	
19. Security Classif. (of this report) Unclassified	20. Security Classif. (of this page) Unclassified	21. No. of Pages 32	22. Price* $3.75

NOMENCLATURE

a_i = design variables for the upper surface,
$i = 1,7$

b_i = design variables for the lower surface,
$i = 1,7$

C_d = section drag coefficient

C_l = section lift coefficient

C_m = section pitching-moment coefficient,
referenced to quarter-chord point

C_p = pressure coefficient, $(p_1-p)/q$

C_p^* = pressure coefficient corresponding to a
local Mach number of 1

c = chord

M = Mach number

p = free-stream static pressure

p_1 = local static pressure

q = free stream dynamic pressure

Re = Reynolds number

$\bar{s}$ = move direction vector

x = chordwise distance

y = vertical distance

α = angle of attack

Subscripts

inv = inviscid

ls = lower surface

max = maximum

min = minimum

us = upper surface

visc = viscous

THE WORLDWIDE FUEL SHORTAGE has prompted new
interest in reducing the fuel consumption of
existing and future aircraft and a logical
place to begin is by reducing drag. At tran-
sonic speeds drag reduction can be accomplished
by eliminating or weakening rapid recompressions
or shock waves over the aircraft surfaces. In
particular, the wing profile can often be
redesigned to achieve drag reduction.

Several methods are available to aid the
designer in developing advanced airfoil sec-
tions (e.g., the hodograph method (1,2),* an
inverse method applied in the physical plane
(3), and a combined inverse-direct method (4).
However, the hodograph procedure is complicated
and its application requires extensive experi-
ence in applied mathematics and theoretical
fluid mechanics. The inverse method requires
an a priori knowledge of the desirable form
of the pressure or velocity distribution, and
constraints are not readily imposed. The
combination inverse-direct method is complicated
and requires a designer in the "loop" to
monitor and enhance the convergence of the
optimization process to a realistic airfoil
shape.

In this report the numerical optimization
design technique (5-8) has been extended to
the design of lifting transonic airfoils. The
numerical optimization design technique uses
two existing computer programs: an optimization
program based on the method of feasible direc-
tions (9) and an aerodynamics analysis program
based on an iterative solution of the full
potential equation for transonic flow (10).
The optimization procedure can be used to
design airfoil sections for any speed regime
from low speed through transonic with geometrir
or aerodynamic constraints. Several examples
of the application of the procedure to the
design of low-drag transonic airfoils are given.
It should be noted that the results presented
here are preliminary and are intended only to
illustrate the usefulness and simplicity of
the technique.

DESIGN METHOD

The program organization of the numerical
optimization design technique used in this

*Numbers in parentheses designate References
at end of paper.

study is shown in Fig. 1. The initial airfoil
required to start each design problem is obtained
by fitting a polynomial to that region of the
airfoil to be modified, or to the entire airfoil
if a complete new profile is desired. The coef-
ficients of such a polynomial are the design
variables perturbed by the optimization program
to achieve the desired design improvement. If
a 6th degree polynomial representation of the
airfoil geometry is used, the coefficients for
the starting airfoil are obtained by fitting the
polynomials to seven points on the upper surface
and to seven points on the lower surface of a
known suitable airfoil section. The coeffi-
cients, along with the Mach number, angle of
attack, and constraints are the required inputs
to start the optimization process.

If the problem being considered is pitching-
moment minimization, the optimization program
perturbs the polynomial coefficients one by one,
returning to the aerodynamics program for evalua-
tion of the pitching moment after each perturba-
tion. After all coefficients have been perturbed
and the direction of change of the pitching
moment has been noted for each polynomial coef-
ficient change, the optimization program then
calculates the partial derivatives (by one-sided
finite difference) of moment with respect to each
polynomial coefficient, thus forming the gradient
of the pitching moment (∇C_m). The direction in
which the polynomial coefficients are changed to
reduce the nose-down pitching moment is $-\nabla C_m$
(the steepest descent direction). The optimiza-
tion program then increments the polynomial
coefficients one to four times in the direction
indicated by $-\nabla C_m$. The program searches in this
direction until the moment starts to increase
(because of nonlinearity in the design space) or
a constraint is encountered. If either of these
possibilities occurs, new gradients are calcu-
lated and a new direction is found that will
decrease pitching moment without violating any
constraints. When a minimum value of pitching
moment is reached with no violated constraints,
the coordinates of the final airfoil are printed,
together with the final pressure distribution
and aerodynamic coefficients.

A graphic presentation of a hypothetical
optimization problem using two design variables
is shown in Fig. 2. Assume that the optimiza-
tion problem to be attempted is minimization
of drag coefficient with constraints on lift
coefficient and airfoil thickness, and with
the airfoil geometry described by the poly-
nomials shown in the figure. In this case,

4

the optimization program is allowed to perturb
only a_1 and a_2 to achieve the desired drag
reduction. This permits only a limited
reshaping of the upper surface. Note that the
thickness constraint is a straight line (that
is, a linear function of the polynomial coef-
ficients) whereas the lift constraint is non-
linear. The optimization program can handle
both linear and nonlinear constraints effici-
ently.

The design space is divided into two
regions, an infeasible region where one or both
constraints are violated, and a feasible region
where no constraints are violated. Minimum
drag in the feasible region is sought. Assumed
starting values of a_1 and a_2 are depicted by
point A. The gradient of drag (∇C_d) is
calculated for this point, giving the direction
of change in a_1 and a_2 as $\bar{s} = -\nabla C_d$. In this
case, both a_1 and a_2 must be decreased to
minimize drag. Movement in direction $\bar{s}$ con-
tinues until the lift constraint is encountered
at point B. At this point, the gradient of
lift (∇C_l) is required along with ∇C_d to define
a new direction $\bar{s}$. Now a_1 must be increased
and a_2 must be decreased to minimize drag by
moving along the lift constraint. The optimum
is shown as the point where the line of constant
drag with least value in the feasible region
intersects the lift constraint.

If the starting values of a_1 and a_2 are
given by point C (Fig. 2), the problem begins
in the infeasible region. Now a direction $\bar{s}$
is determined that moves toward the feasible
region with a minimum increase in drag, while
overcoming the violated lift constraint. Such
a move requires an increase in both a_1 and a_2.
When the feasible region is reached, a direction
$\bar{s}$ is then determined that will move along the
lift constraint until the optimum is attained.
A more complete discussion of airfoil design
by numerical optimization is given in ref-
erence 8.

DESIGN RESULTS AND DISCUSSION

All design problems considered during this
study consisted of modifying the upper surface
of an existing airfoil section to achieve
transonic drag reduction. The equation used
to describe that portion of the upper surface
to be modified is the following cubic equation:

$$y = a_1(x/c)^{a_4} + k(x/c) + a_2(x/c)^2 + a_3(x/c)^3 \quad (1)$$

The coefficient, k, is used to match ordinates at the chordwise station where the forward region of the airfoil to be modified ends and the fixed aft region begins. When the entire upper surface is to be modified, the coefficient, k, is used to fix the trailing edge bluntness. The design variables are the coefficients, a_1-a_3, and the exponent, a_4. The starting value of a_4 was 0.5 for all initial airfoil sections considered. The final value of a_4 depends on the amount of leading edge bluntness required to achieve drag reduction. Each airfoil modification reported here was found to need more leading edge bluntness than exhibited by the starting airfoil to achieve the desired drag reduction and hence the final value of a_4 was less than 0.5 in each case.

While substantial drag reductions were achieved by using equation (1), the development of shock-free sections was difficult because of the restricted class of sections that can be described by such an equation. Additional work is needed to obtain more general geometric representations for transonic airfoil design. In particular, equations are needed that will allow decoupling of various regions of the airfoil surface without permitting waviness to develop. The inability to develop shock-free sections may not be a serious limitation of the method, however, since the off-design characteristics of such sections are often poor in comparison to weak-shock sections. In each case presented here the shock strength was sufficiently weakened to prevent shock-induced boundary layer separation from occurring at the design condition (i.e., the shock-Mach number was reduced to at least 1.2 in each case).

In reference to the figures cited below, only upper surface pressure distributions are shown when the presentation is clarified by omitting lower surface pressures. (There were only slight changes in the lower surface pressures when the upper surface was modified.)

CASE I. UPPER SURFACE MODIFICATION OF AN APPROXIMATE NACA 6-SERIES PROFILE – The results of modifying the upper surface of an airfoil to achieve drag reduction at $M = 0.7$ are shown in Fig. 3. The initial airfoil is an approximation to a 13-percent thick NACA 6-series section. The lower surface is exact and the upper surface is represented by equation (1). The drag coefficient given in the figure is

6

obtained by a surface pressure integral and
represents the drag due to shock losses in an
inviscid flow. Note that the drag coefficient
is reduced to approximately one-fourth that of
the initial airfoil. The drag reduction is
accompanied by a reduction in nose-down pitching
moment, a small loss in lift, and a redistri-
bution of the area contained within the profile
contour. A constraint on the cross-sectional
area ("volume") of the profile prevented
further thinning of the section to achieve the
drag reduction. Note the substantial reduction
in shock strength and the forward movement of
the shock position.

The aerodynamic characteristics of the two
airfoils of Fig. 3, corrected for viscosity,
are shown at Reynolds numbers of 1.3×10^6
and 20×10^6 in Figs. 4(a) and 4(b), respec-
tively. The boundary layer characteristics
were calculated by a theory described in ref-
erence 10. This theory uses an inviscid pres-
sure distribution as input to the von Karman
momentum equation which, when integrated,
gives the boundary layer displacement thickness.
This displacement thickness is smoothed and
added to the airfoil contour to account for a
turbulent boundary layer. The displacement
thickness correction is computed iteratively
with the flow calculation. As expected, the
lift and pitching moment coefficients show
the typical decambering effect of the boundary
layer; namely, the coefficients for viscous
flow are smaller than the corresponding coef-
ficients for inviscid flow. Note that the
drag reduction due to modification of the
airfoil contour is smaller when the boundary
layer correction is included in the calculation;
nevertheless, a substantial reduction still is
achieved. The aerodynamic coefficients shown
in Fig. 4(b) at a Reynolds number of 20×10^6
are somewhat closer to the corresponding
inviscid values because of the smaller boundary
layer thickness at the higher Reynolds number.
Again, a substantial drag reduction is noted.

A graph of C_d vs Mach number at $\alpha = 0°$
for the initial and final profiles of Fig. 3
is shown in Fig. 5 for a Reynolds number of
20×10^6. The drag divergence Mach number is
increased by approximately 0.04 by the contour
reshaping shown in Fig. 3. It is interesting
to note that this type of re-contouring to
reduce shock drag at transonic speeds does not
produce a drag penalty for subsonic flow or a
more rapid drag rise above the design Mach
number ($M = 0.7$).

7

Plots of low speed (M = 0.1) pressure
distributions for α = 10° are given in Fig. 6
for both of the airfoils shown in Fig. 3. The
low speed aerodynamic characteristics were
evaluated for the airfoil shown in Fig. 6 and
for the next two profile modifications (Figs. 7
and 11) to investigate the compatibility of
section re-contouring for transonic drag reduc-
tion with low speed, high lift requirements.
Note that the pressure peak near the leading
edge on the upper surface is reduced by more
than a factor of 2 by increasing the leading
edge bluntness of the 'initial' airfoil shown
in Fig. 3. Moreover, the adverse pressure
gradient following the leading edge pressure
peak is substantially reduced, thereby improving
maximum lift and low-speed handling.

CASE II.   FORWARD UPPER SURFACE MODIFICA-
TION OF AN APPROXIMATE NACA 6-SERIES PROFILE -
The results of modifying the forward 35 percent
of the upper surface of a 12-percent thick NACA
6-series section to reduce shock drag at M = 0.72
are shown in Fig. 7. Again, a substantial
reduction in drag is achieved along with a
smaller nose-down pitching moment and little
change in lift coefficient. The slight irregu-
larity in the pressure distribution near the
38-percent chord station is due to a slight
mismatch in the first derivative of the contour
at the point where the forward section described
by equation (1) joined the fixed aft section
of the airfoil. Such irregularities can arise
because the only boundary conditions imposed
on the geometry of the upper surface were
matched ordinates at the end of the forward
section.
The aerodynamic characteristics of the air-
foil sections of Fig. 7, corrected for viscosity,
are shown in Figs. 8(a) and 8(b) for Reynolds
numbers of 1.3×10^6 and 20×10^6, respectively.
As noted for the preceding case (Figs. 3 and 4),
the lift and pitching moment coefficients are
reduced due to the decambering effect of the
boundary layer. The reduction in drag is
smaller when viscous effects are included but
still large enough to warrant consideration of
such contour modification for retrofit of
existing aircraft.
The effect of Mach number on the drag
characteristics of the airfoils of Fig. 7 is
shown in Fig. 9 for a Reynolds number of
20×10^6. As for the preceding case (Figs.
3-6), no drag penalty is incurred at subcritical

8

Mach numbers by the type of contour modifications
considered here. The drag divergence Mach number
is increased by appr ximately 0.02 with similar
drag rise character.stics above the design point
(M = 0.72) for both airfoil sections.

The low speed pressure distributions at
high angles of attack for the two sections of
Fig. 7 are shown in Fig. 10. As noted in the
previous case (Figs. 3-6), the increased
leading edge bluntness of the modified section
produced a reduced pressure peak, a smaller
adverse pressure gradient and a rearward shift
of the pressure peak. All these factors should
increase the maximum lift coefficient and
improve the low speed handling of aircraft
incorporating this airfoil modification.

CASE III. FORWARD UPPER SURFACE MODIFICA-
TION OF THE NACA 23015 PROFILE - The results
of a forward upper surface contour modification
designed to reduce the shock drag of the NACA
23015 airfoil section at M = 0.7 and α = 0° are
shown in Fig. 11. In this case the initial
airfoil shown in the figure and the correspond-
ing upper surface pressure distribution represent
the exact NACA 23015 profile rather than an
approximation obtained by using equation (1),
as was done for the initial airfoil in the two
preceding NACA 6-series airfoil modifications.
In this case the modified section is almost
shock-free (C_d = 0.0005) and exhibits nearly
the same pitching moment and lift coefficients
as the original NACA 23015 section. The desired
drag reduction was achieved with a smaller
contour change than that made in the two pre-
ceding cases because the initial shock was
weaker (compare Figs. 3 and 7 with Fig. 11).

The aerodynamic characteristics of the
original and of the modified 23015 sections,
corrected for viscosity, are shown in Fig. 12
for a Reynolds number of 10×10^6. Again, the
same trend as noted for the two previous NACA
6-series modifications is noted: namely, the
lift and pitching moment coefficients are
reduced, relative to the inviscid values, due
to viscous effects, and the percent reduction
in drag is smaller.

The effect of Mach number on the drag
characteristics of the modified and original
NACA 23015 sections is shown in Fig. 13 for a
Reynolds number of 20×10^6. The improved
drag rise Mach number and drag rise character-
istics exhibited by the modified 23015 section
are similar to those noted earlier for the

9

modified 6-series sections (Figs. 5 and 9).
However, the subsonic drag of the modified
23015 section is predicted to be somewhat less
than that of the original NACA 23015 profile.

The low speed, high lift characteristics
of the modified 23015 profile require a more
careful analysis than the modified 6-series
sections shown previously because the original
NACA 23015 airfoil section exhibits one of
the highest maximum lift coefficients of all
NACA profiles that have similar design lift
coefficients (11). The type of profile modifi-
cation used in this study can generally be
relied upon to improve the high lift character-
istics of 6-series airfoils at low speed because
most 6-series profiles have relatively small
leading edge radii. However, when such modifi-
cations are applied to NACA 4- and 5- digit
sections to reduce drag at transonic speeds,
the low speed, maximum lift characteristics
of the modified profiles may incur a slight
penalty. Such a penalty can often be minimized
or avoided, if the high lift characteristics
are considered during the optimization process,
by careful application of constraints on the
design.

The inviscid, low speed pressure distri-
butions for the NACA 23015 section and modified
section are shown in Figs. 14 and 15, respec-
tively, at four angles of attack from $0°$ to $15°$.
Analysis of these pressure distributions shows
two interesting facts: first, the modified
profile exhibits greater suction pressures
than the original NACA 23015 section at all
angles of attack shown, except at $0°$; and
second, the rate of growth of $C_{p_{min}}$ with angle
of attack is smaller for the modified section
than for the original section. This latter
fact is illustrated more clearly in Fig. 16,
which shows a graph of the ratio of minimum
pressure coefficient for the modified section
to minimum pressure coefficient for the original
section vs angle of attack. Note, that the
ratio decreases above $\alpha = 7°$. Since the
stalling angle for the NACA 23015 section is
between $15°$ and $18°$, depending on Reynolds
number (11), it is possible that the pressure
coefficient ratio may reach a value of 1.0
before stall, and hence the maximum lift
coefficient for the two profiles may be similar.
A wind tunnel test would be the only means of
providing positive evaluation of the high
lift characteristics of the two profiles.

CASE IV. FORWARD UPPER SURFACE MODIFICA-
TION OF THE NACA 64A109 PROFILE - The final
drag minimization problem considered in this
study was modification of the forward upper
surface of the NACA 64A109 section for M = 0.82
(Fig. 17). The results of this modification are
similar to those shown for the 6-series sections
shown in Figs. 3 and 7; that is, the drag is
substantially reduced along with a reduction in
nose-down pitching moment and little change in
lift coefficient. The off-design character-
istics and low speed, high lift characteristics
were not evaluated because of time limitations
and the fact that the trends would be expected
to be similar to those shown for the previous
6-series modifications. The initial profile and
corresponding pressure distribution shown in
the figure are those of the exact NACA 64A109
profile.

CONCLUDING REMARKS

A technique for achieving drag reduction
of airfoil sections at transonic speed was
demonstrated. When the method is applied to
drag reduction of NACA 6-series sections, or
to other profiles with small leading edge
radii, the reduced drag is generally accompanied
by a reduction in nose-down pitching moment,
little change in lift coefficient for the
design condition, and improved low speed, high
lift characteristics.
When NACA 5-digit sections, or other
profiles with larger leading edge radii, are
modified to achieve drag reduction at transonic
speeds, it was again found that the nose-down
pitching moment was reduced; the lift coefficient
remained about the same at the design condition.
However, a more careful analysis of the low
speed, high lift characteristics is required
and some additional re-contouring of the profile
may be required to insure adequate low speed
aerodynamics.
Further work is needed to achieve more
flexibility in the geometric representation
used with the numerical optimization technique
so that a wider range of modifications can be
achieved.
Experimental verification of the type of
modifications developed during this study is
required before such designs can be considered
for retrofit of existing aircraft or used in
new aircraft.

11

The off-design characteristics of the four
airfoil modifications developed during this
study were good. Furthermore, it is expected
that such off-design behavior is typical of the
type of low drag, transonic airfoil section
generated by the design technique presented in
this report.

In all cases the modifications were devel-
oped by use of an inviscid aerodynamic theory
to reduce computational cost. The aerodynamic
characteristics of the initial and final pro-
files were verified by use of a theory that
includes viscosity corrections.

A typical airfoil modification, including
re-contouring by numerical optimization,
verification of design by use of a theory
corrected for viscosity, and evaluation of
low speed, high lift characteristics required
approximately 20 min of CPU time on a CDC 7600
computer.

REFERENCES

1. F. Bauer, P. Garabedian, and D. Korn,
Lecture Notes in Economics and Mathematical
Systems. "Supercritical Wing Sections," Vol.
66, Springer-Verlag, 1972.

2. G. Y. Nieuwland, "Transonic Potential
Flow Around a Family of Quasi-Elliptical Aerofoil
Sections." National Aerospace Laboratory,
Technical Report T. 172, 1967.

3. B. Arlinger, "An Exact Method of Two
Dimensional Airfoil Design." Saab TN 67, 1970.

4. Joseph L. Steger and John M. Klineberg,
"A Finite Difference Method for Transonic
Airfoil Design." AIAA Journal, Vol. 11, No. 5,
May 1973.

5. Raymond M. Hicks, Earll M. Murman,
and Garret N. Vanderplaats, "An Assessment of
Airfoil Design by Numerical Optimization."
NASA TM X-3092, 1974.

6. Raymond M. Hicks and Garret N.
Vanderplaats, "Application of Numerical
Optimization to the Design of Low-Speed Air-
foils." NASA TM X-3213, 1975.

7. Raymond M. Hicks and Garret N.
Vanderplaats, "Design of Low-Speed Airfoils
by Numerical Optimization." SAE Paper 750524,
1975.

8. Garret N. Vanderplaats, Raymond M.
Hicks, and Earll M. Murman, "Application of
Numerical Optimization Techniques to Airfoil
Design." NASA SP-347, 1975.

9. Garret N. Vanderplaats, "CONMIN-A Fortran Program for Constrained Function Minimization." NASA TM X-62,282, Aug. 1973.

10. F. Bauer, P. Garabedian. D. Korn, and A. Jameson, Lecture Notes in Economics and Mathematical Systems. "Supercritical Wing Sections II," Vol. 108, Springer-Verlag, 1975.

11. I. H. Abbott, A. E. von Doenhoff, and L. S. Stivers Jr., "Summary of Airfoil Data." NACA Report No. 824, 1945.

AERODYNAMICS PROGRAM

OPTIMIZATION PROGRAM

INPUT INITIAL AIRFOIL
$(a_1 \cdots a_7, b_1 \cdots b_7)$ AND
CONSTRAINTS

$y_{US} = a_1 \sqrt{x} + a_2 x + \cdots + a_7 x^6$

$y_{LS} = b_1 \sqrt{x} + b_2 x + \cdots + b_7 x^6$

PERTURB $a_1 \cdots a_7, b_1 \cdots b_7$ AND

CALCULATE $\dfrac{\partial c_m}{\partial a_1} \cdots \dfrac{\partial c_m}{\partial a_7}, \dfrac{\partial c_m}{\partial b_1} \cdots \dfrac{\partial c_m}{\partial b_7}$

$\left(\dfrac{\partial c_m}{\partial a_1} \cdots \dfrac{\partial c_m}{\partial b_7} \right)$

CALCULATE C_m FOR EACH
PERTURBATION OF $a_1 \cdots b_7$

|4 TIMES

FORM GRADIENT ∇C_m =
AND GRADIENT OF ANY
ACTIVE CONSTRAINTS

CHANGE $a_1 \cdots a_7, b_1 \cdots b_7$ TO
MINIMIZE C_m WITHOUT VIOLATING
ANY CONSTRAINTS

CALCULATE C_m FOR NEW
VALUES OF $a_1 \cdots a_7, b_1 \cdots b_7$

1 TO 4 TIMES

C_m IS MINIMUM
WITH NO VIOLATED
CONSTRAINTS

C_m IS NOT MINIMUM

OUTPUT FINAL AIRFOIL WITH PRESSURE
DIST. AND C_L, C_D, C_m

x

y

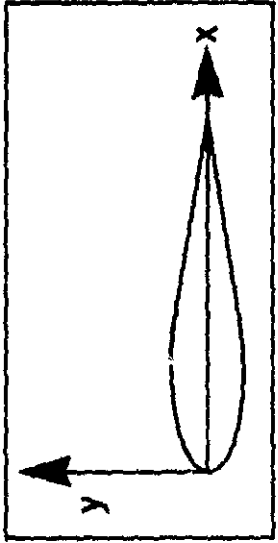Fig. 1 - Program organization

$$Y_u = a_1\sqrt{x} + a_2 x + \cdots + a_7 x^6$$
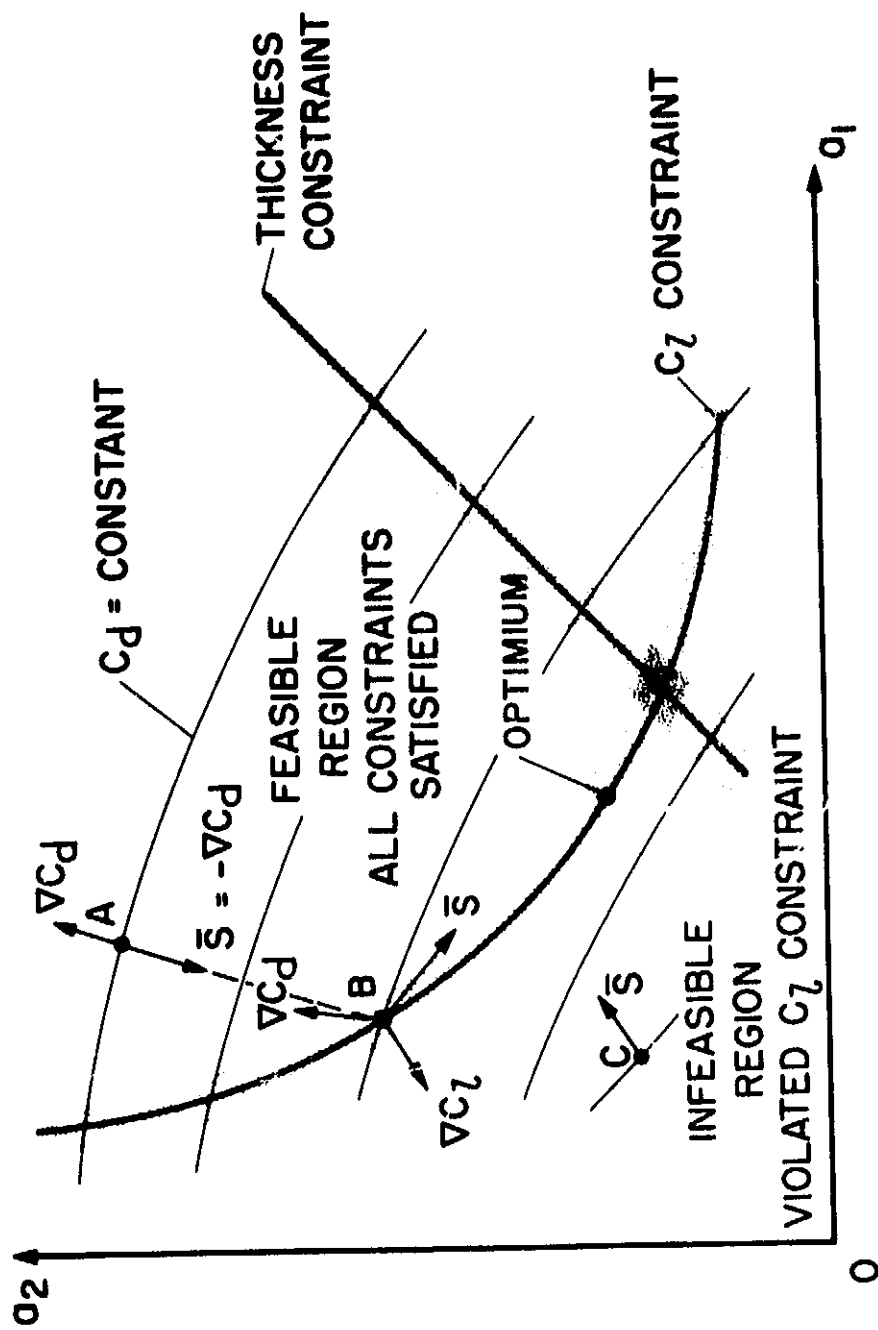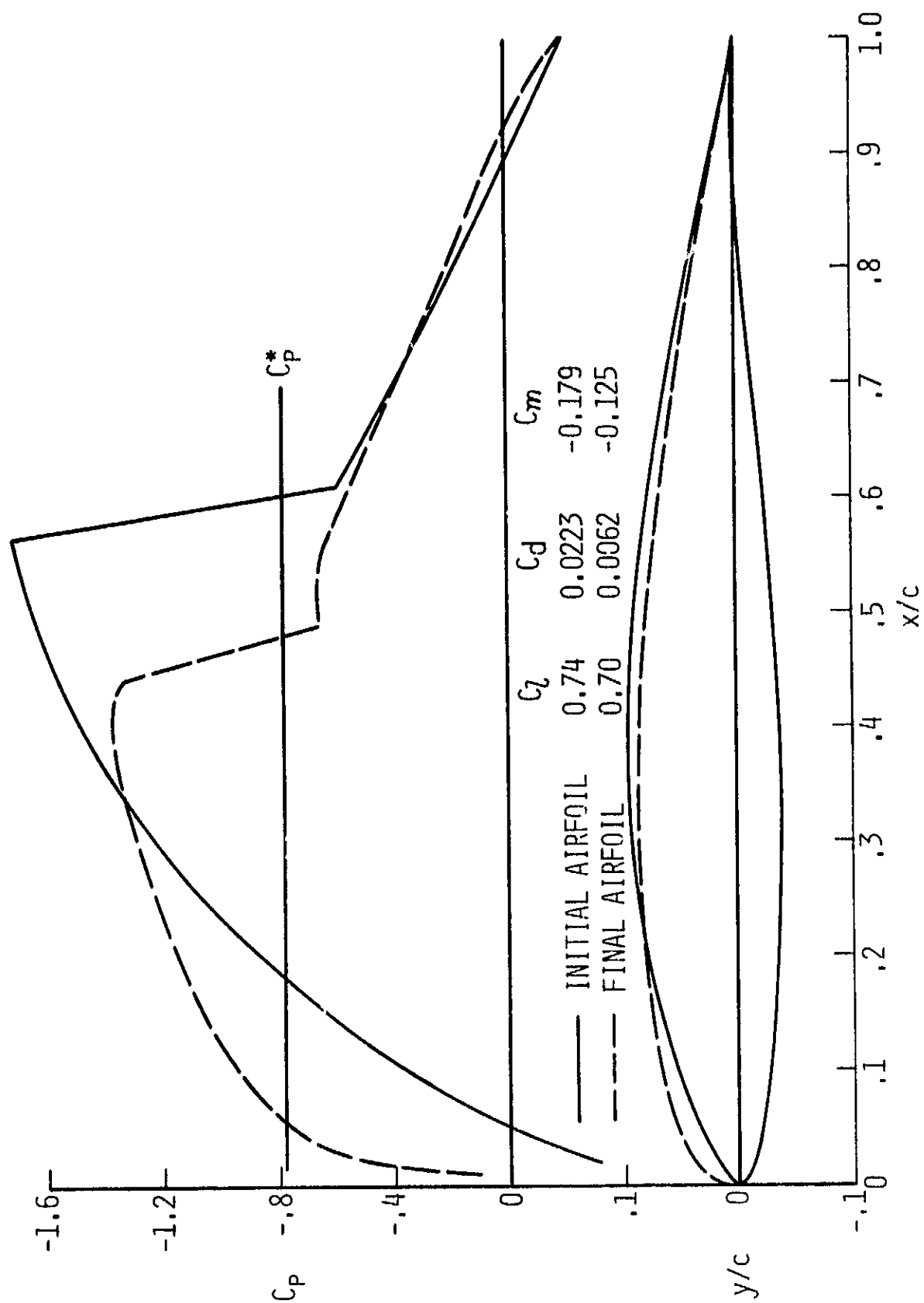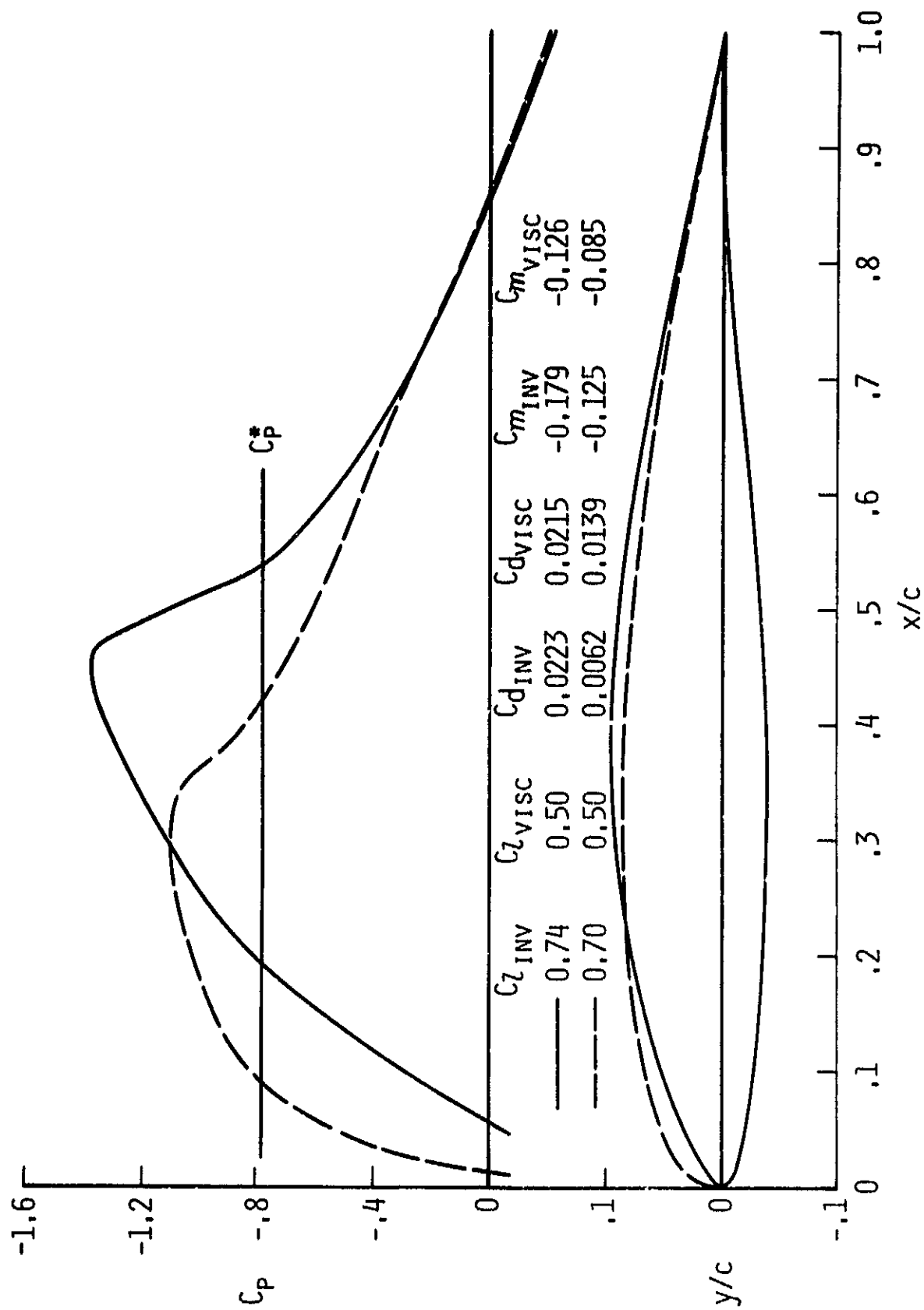$$y_L = b_1\sqrt{x} + b_2 x + \cdots + b_7 x^6$$

THICKNESS CONSTRAINT

C_l CONSTRAINT

C_d = CONSTANT

∇C_d

A

$\bar{S} = -\nabla C_d$

FEASIBLE REGION
ALL CONSTRAINTS SATISFIED

∇C_d

B

OPTIMIUM

$\bar{S}$

∇C_l

C_l

$\bar{S}$

INFEASIBLE REGION
VIOLATED C_l CONSTRAINT

a_1

a_2

O

Fig. 2 – Two-variable design problem

Fig. 3 – Inviscid drag minimization; M = 0.70, $i = 0°$

	C_l	C_d	C_m
INITIAL AIRFOIL	0.74	0.0223	-0.179
FINAL AIRFOIL	0.70	0.0062	-0.125

	$c_{l_{INV}}$	$c_{l_{VISC}}$	$c_{d_{INV}}$	$c_{d_{VISC}}$	$c_{m_{INV}}$	$c_{m_{VISC}}$
	0.74	0.50	0.0223	0.0215	-0.179	-0.126
	0.70	0.50	0.0062	0.0139	-0.125	-0.085

(a) Re = 1.3×10^6

Fig. 4 - Aerodynamic characteristics of the airfoils shown in figure 3 with boundary-layer correction; M = 0.7, α = 0°

$c_{l_{INV}}$	$c_{l_{VISC}}$	$c_{d_{INV}}$	$c_{d_{VISC}}$	$c_{m_{INV}}$	$c_{m_{VISC}}$
0.74	0.56	0.0223	0.0191	−0.179	−0.135
0.70	0.54	0.0062	0.0095	−0.125	−0.092
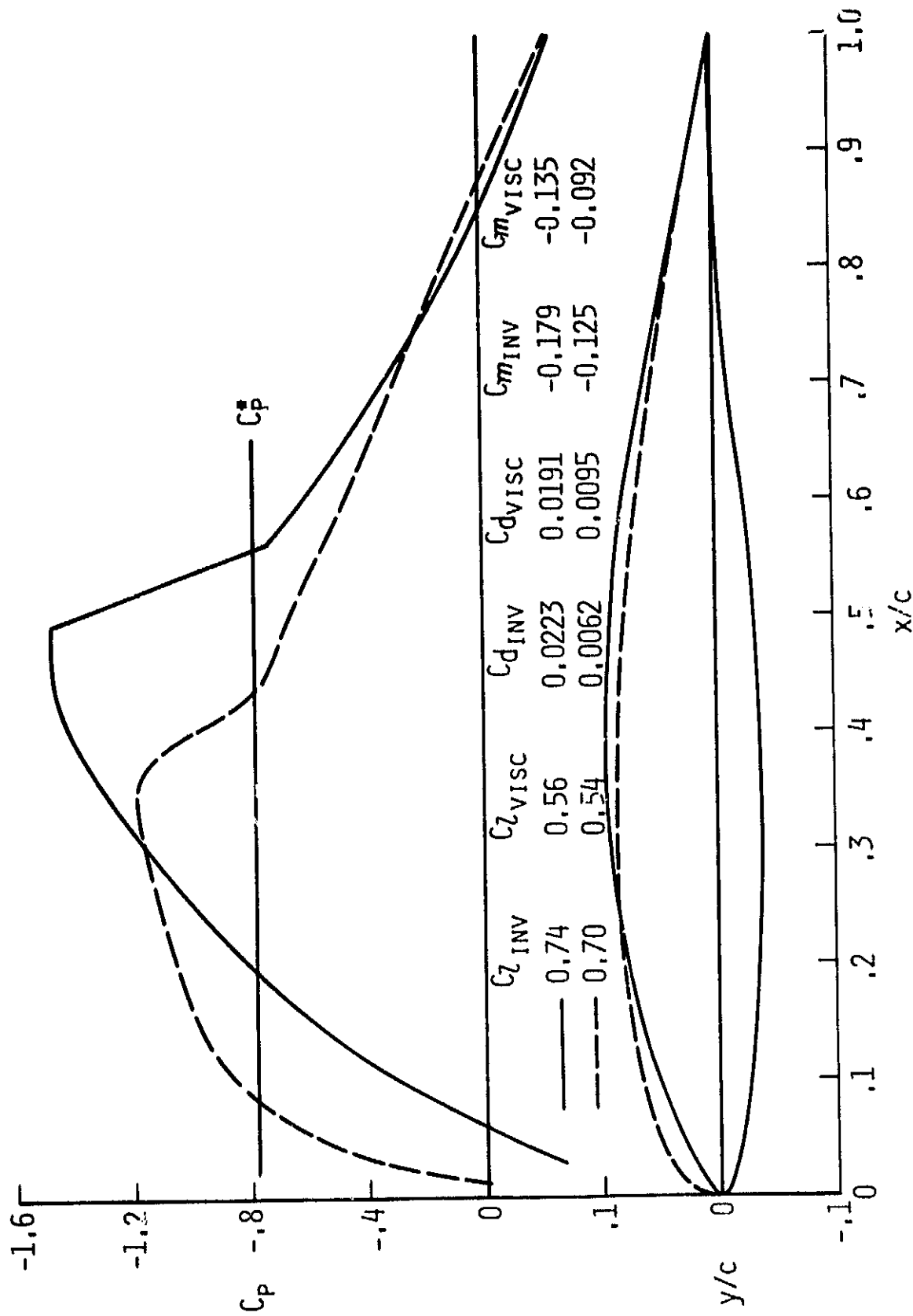
(b) Re = 20×10^6

Fig. 4 – Concluded
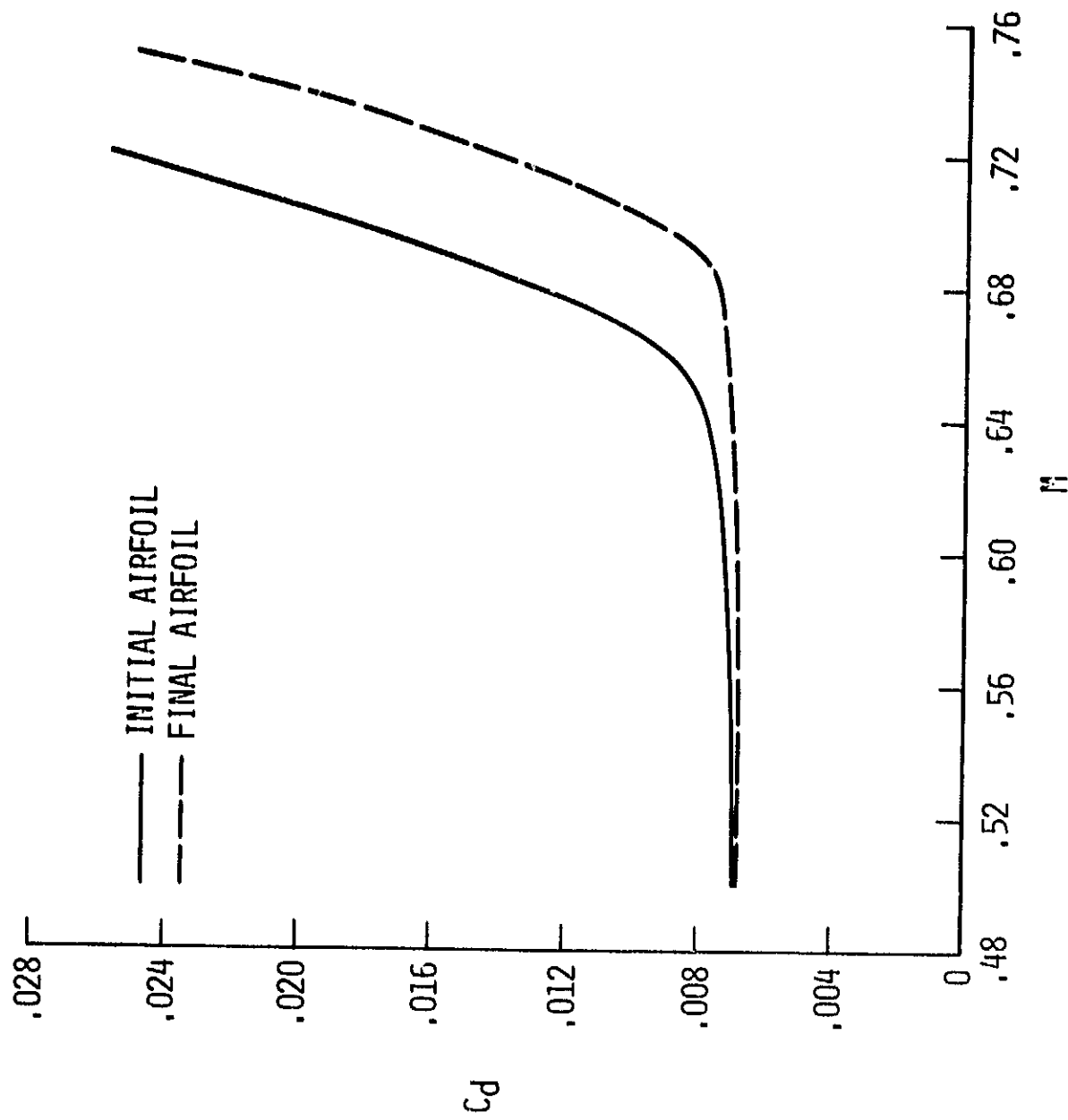
Fig. 5 – Mach number effect on the drag characteristics of the airfoils shown in figure 3; Re = 20×10^6, $\alpha = 0°$
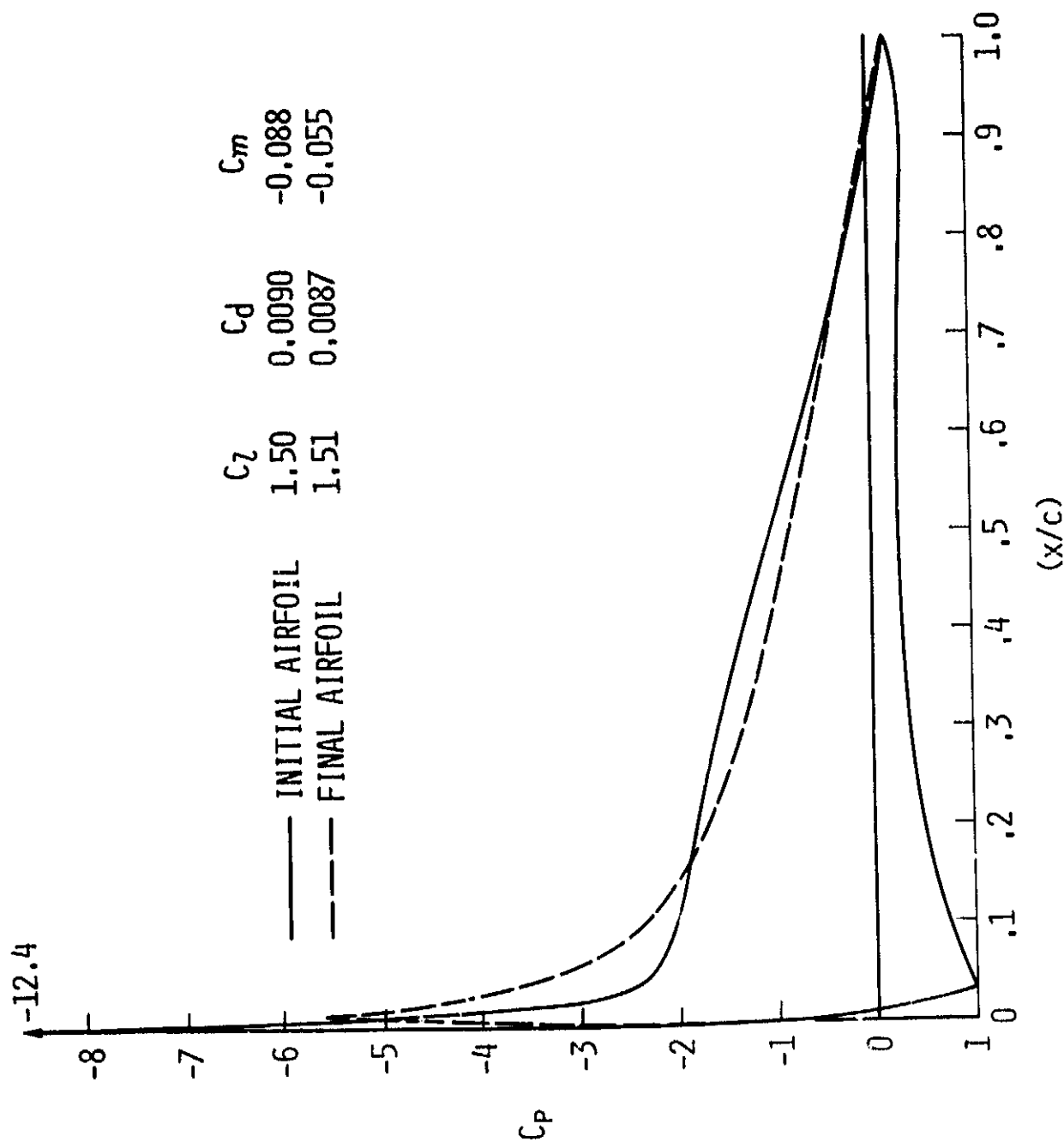
Fig. 6 – Low speed pressure distributions for
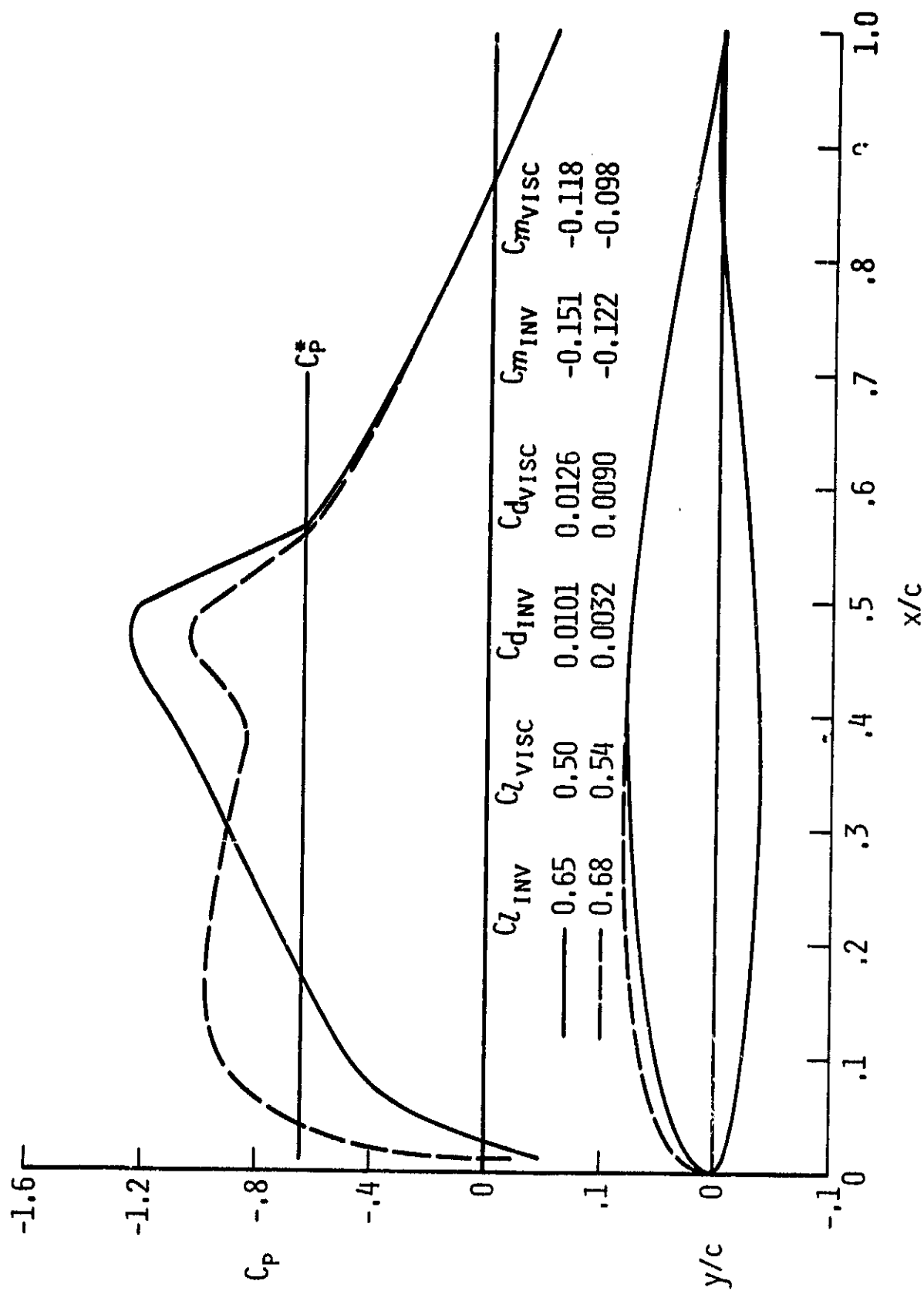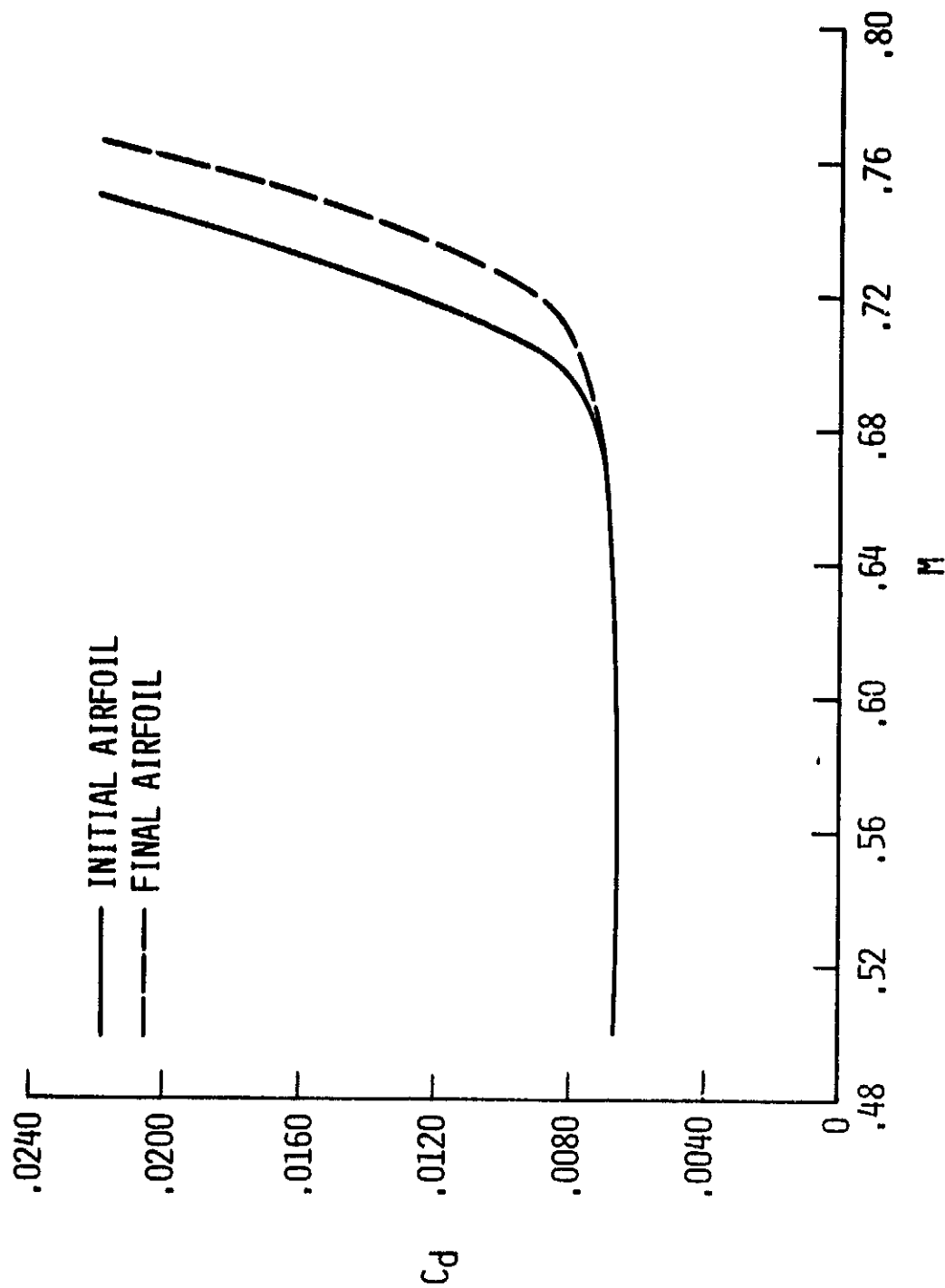the airfoils shown in figure 3; M = 0.1,
Re = 10×10^6, $\alpha = 0°$

	c_l	c_d	c_m
INITIAL AIRFOIL	1.50	0.0090	-0.088
FINAL AIRFOIL	1.51	0.0087	-0.055

	C_l	C_d	C_m
INITIAL AIRFOIL	0.65	0.0101	-0.151
FINAL AIRFOIL	0.68	0.0032	-0.122
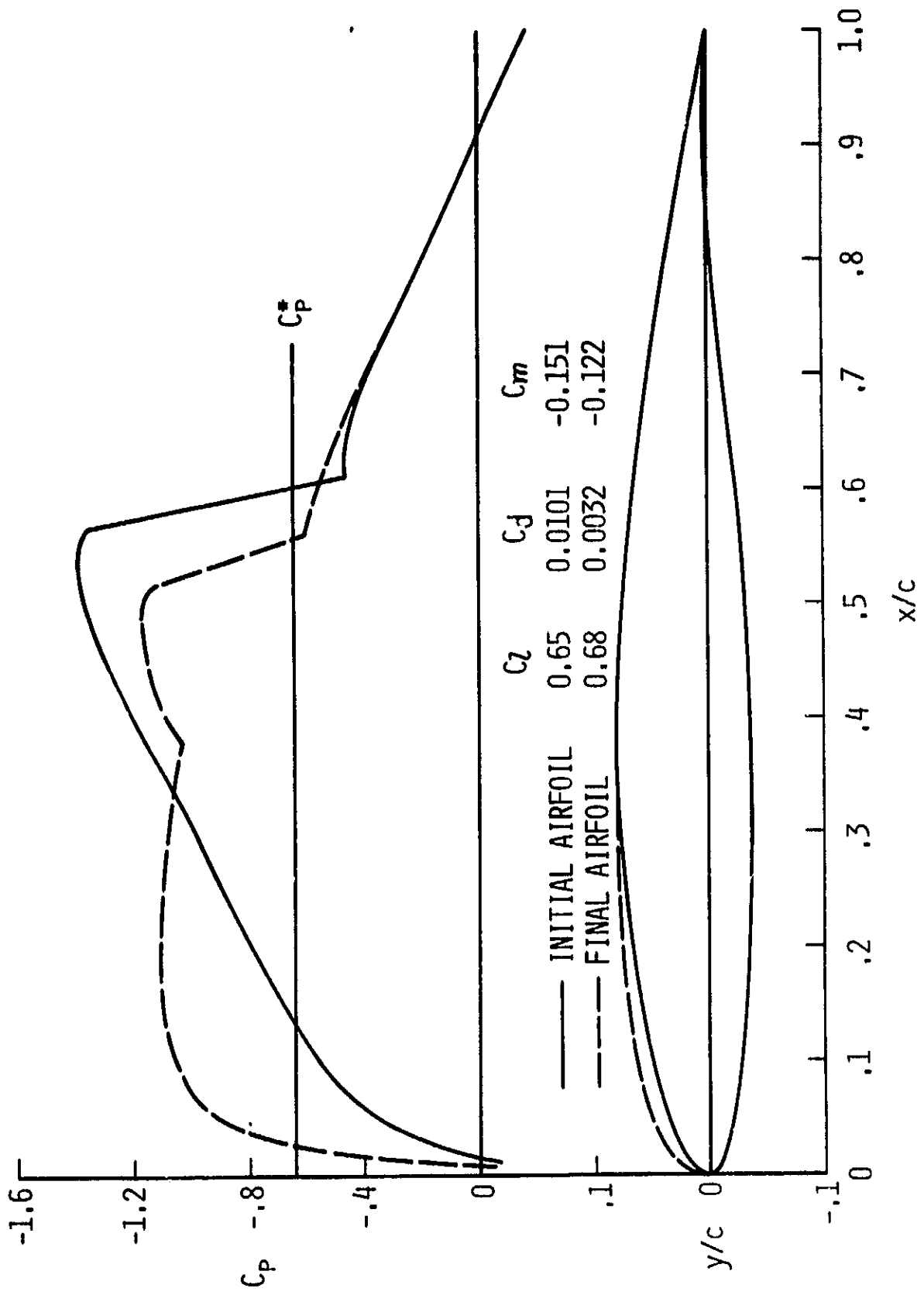
Fig. 7 – Inviscid drag minimization; M = 0.72, $\alpha = 0°$
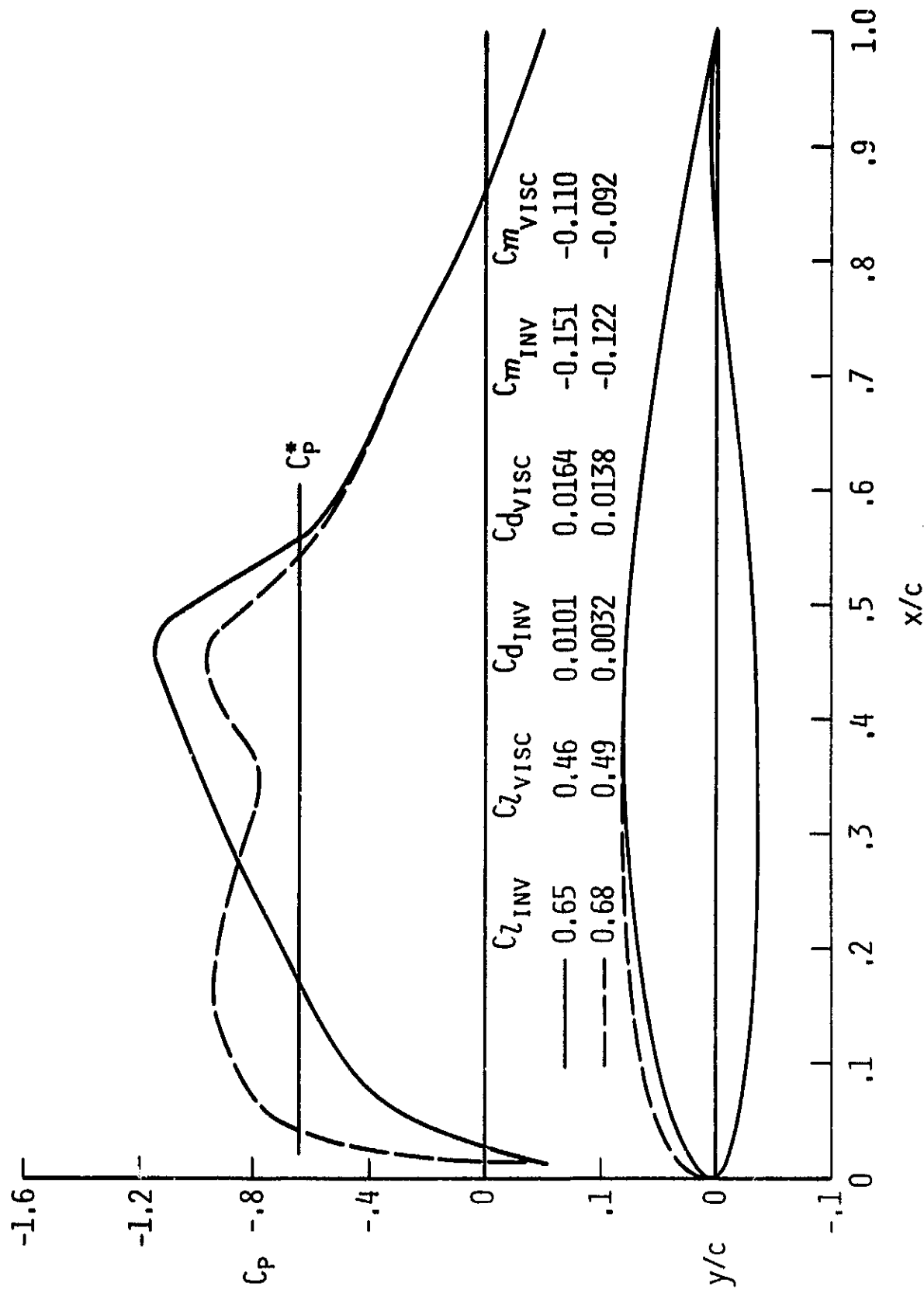
Fig. 8 — Aerodynamic characteristics of the airfoils shown in figure 7 with boundary-layer correction; $M = 0.72$, $\alpha = 0°$

(a) $Re = 1.3 \times 10^6$

	$C_{l_{INV}}$	$C_{l_{VISC}}$	$C_{d_{INV}}$	$C_{d_{VISC}}$	$C_{m_{INV}}$	$C_{m_{VISC}}$
	0.65	0.50	0.0101	0.0126	-0.151	-0.118
	0.68	0.54	0.0032	0.0090	-0.122	-0.098

(b) Re = 20×10^6

Fig. 8 - Concluded

Fig. 9 - Mach number effect on the drag characteristics of the airfoils shown in figure 7; $Re = 20 \times 10^6$, $\alpha = 0°$
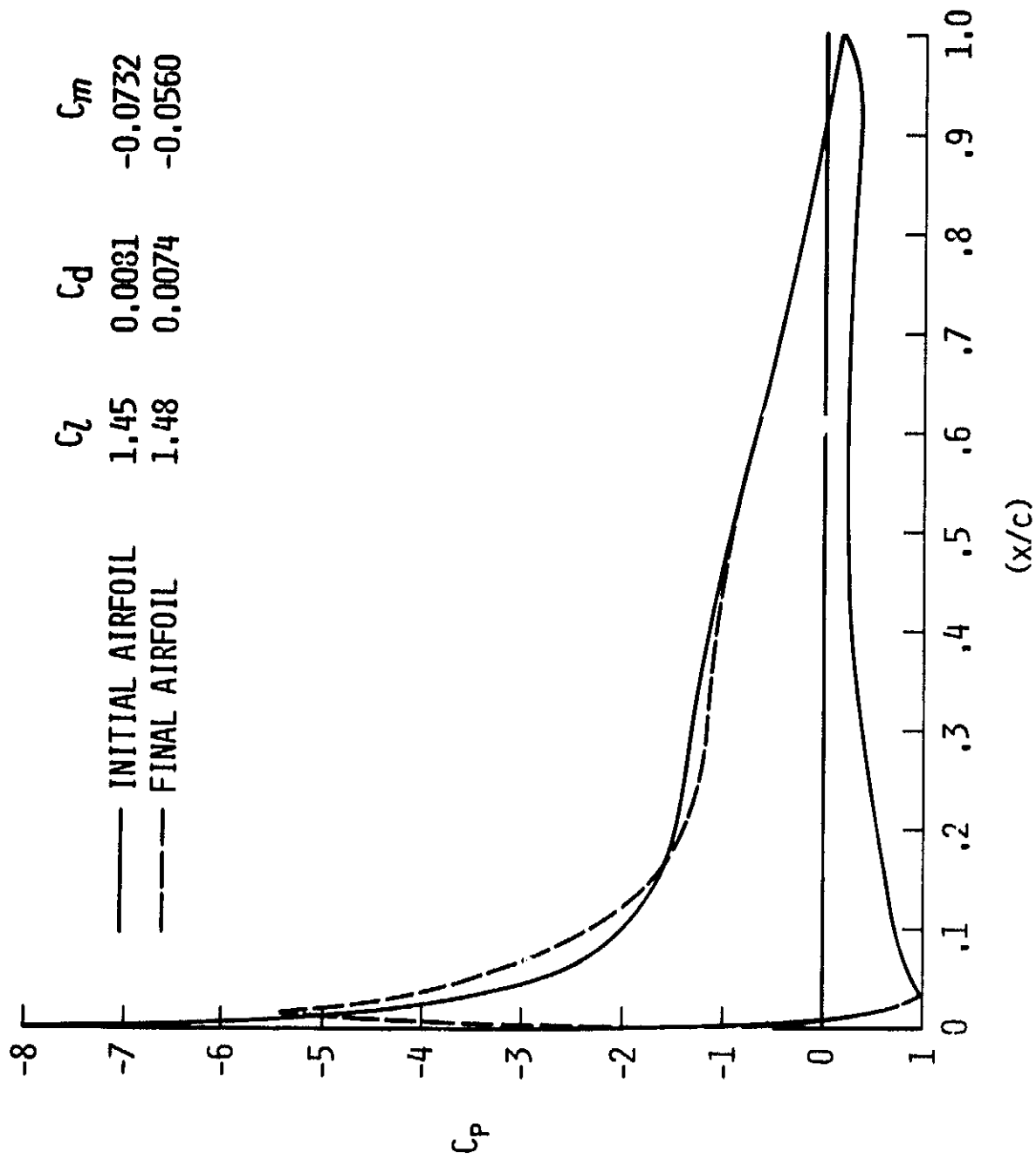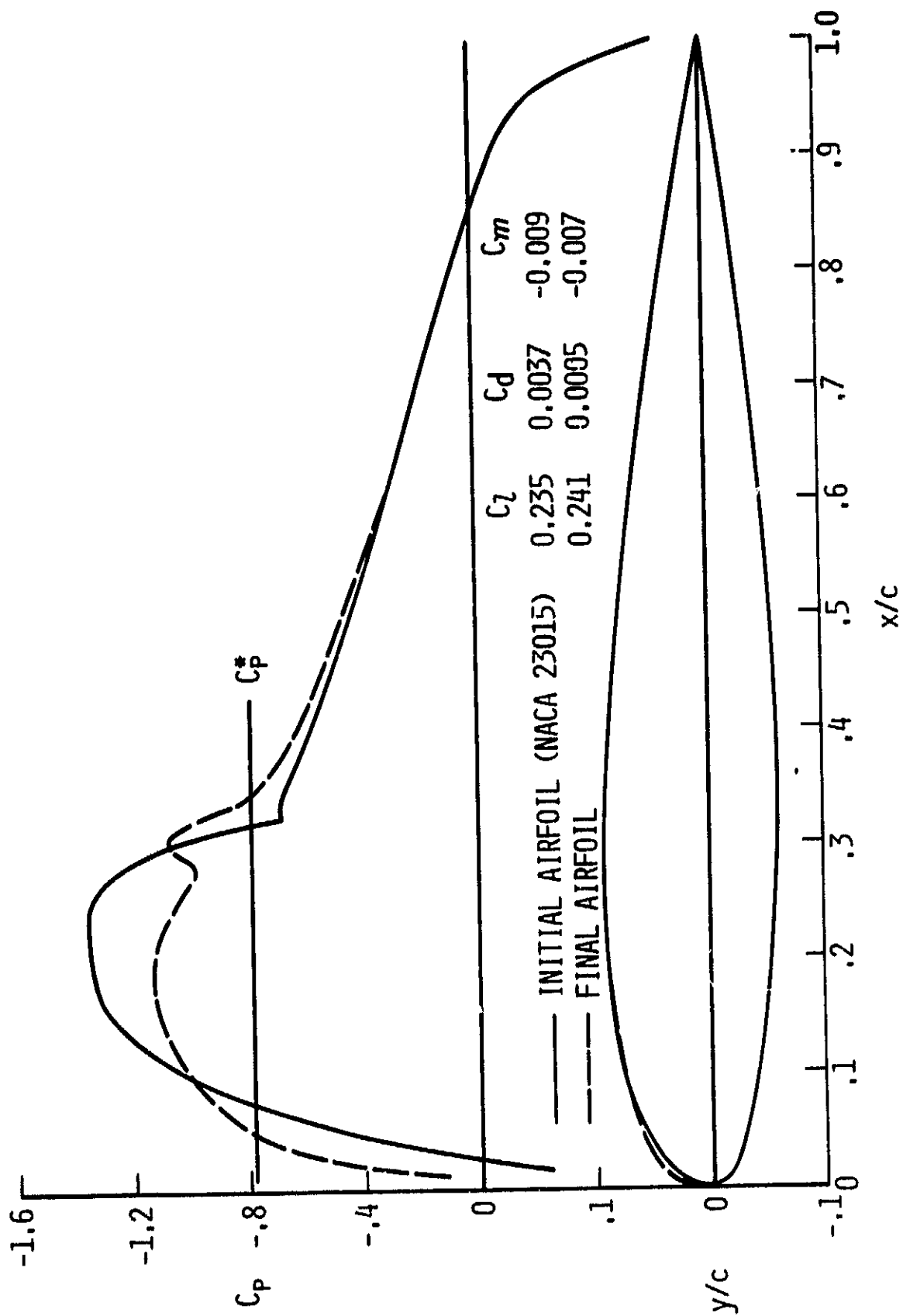
INITIAL AIRFOIL

FINAL AIRFOIL

Fig. 10 – Low speed pressure distributions for the airfoils shown in figure 7; $M = 0.1$, $Re = 10 \times 10^6$, $\alpha = 10°$

	C_l	C_d	C_m
INITIAL AIRFOIL	1.45	0.0031	-0.0732
FINAL AIRFOIL	1.48	0.0074	-0.0560

Fig. 11 - Inviscid drag minimization; M = 0.7, α = 0°

	$c_{l_{INV}}$	$c_{l_{VISC}}$	$c_{d_{INV}}$	$c_{d_{VISC}}$	$c_{m_{INV}}$	$c_{m_{VISC}}$
	0.235	0.135	0.0037	0.0099	-0.009	0.005
	0.241	0.103	0.0005	0.0079	-0.007	0.016

—— INITIAL AIRFOIL (NACA 23015)
— — FINAL AIRFOIL
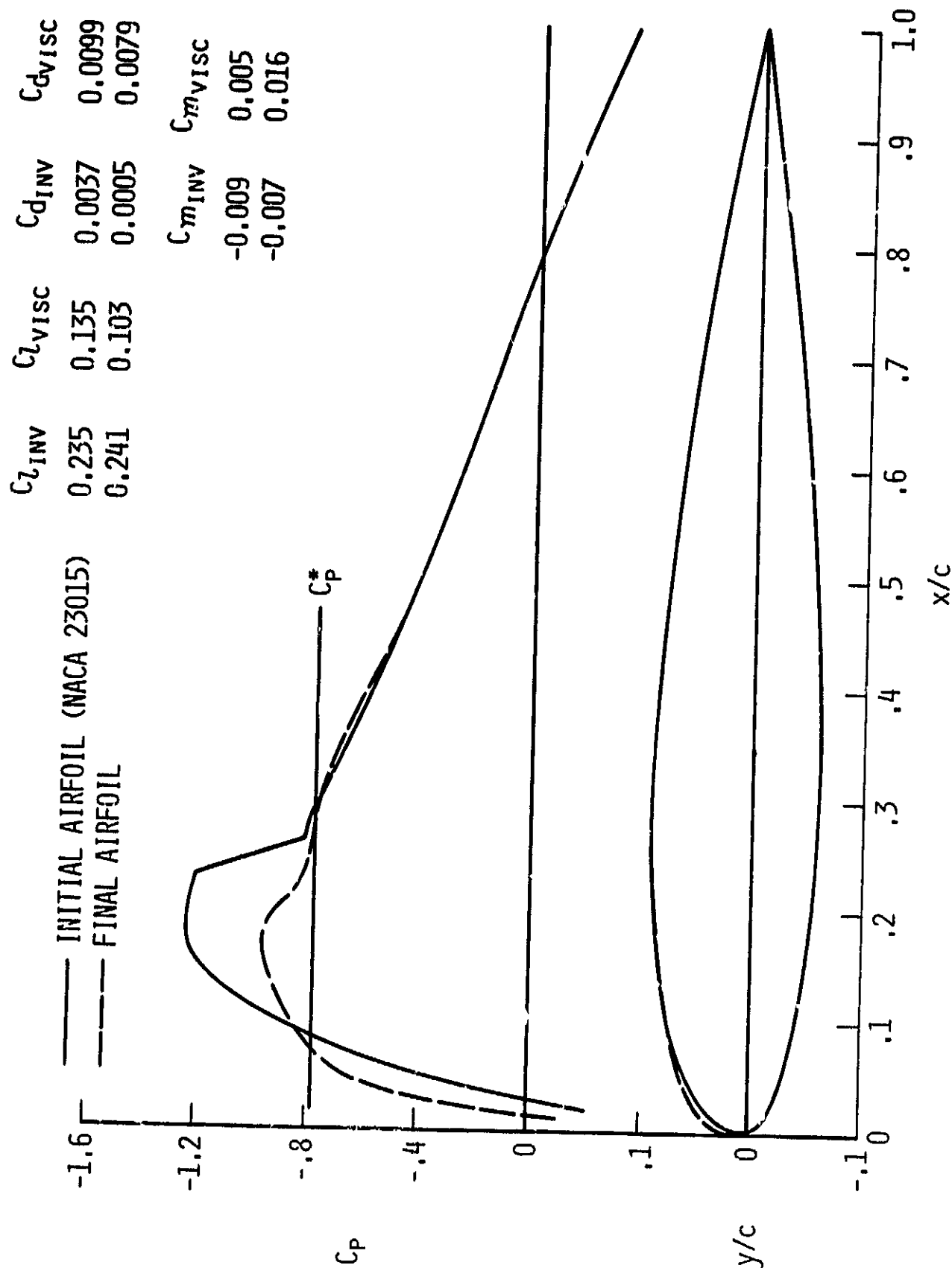
Fig. 12 – Aerodynamic characteristics of the
airfoils shown in figure 11 with boundary-
layer correction; $M = 0.7$, $Re = 10 \times 10^6$,
$\alpha = 0°$,
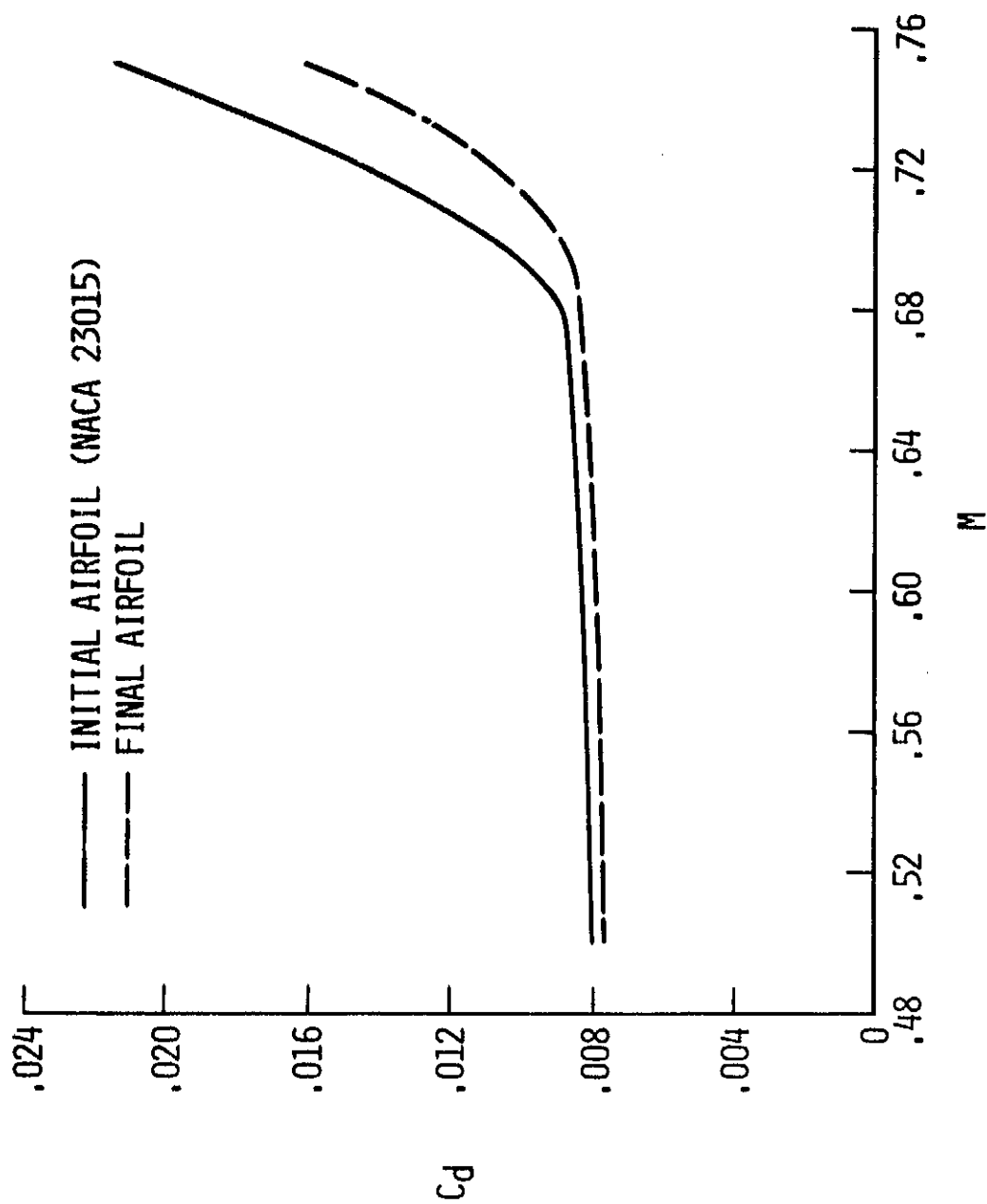
Fig. 13 – Mach number effect on the drag characteristics of the airfoils shown in figure 11; Re = 20×10^6, $\alpha = 0°$
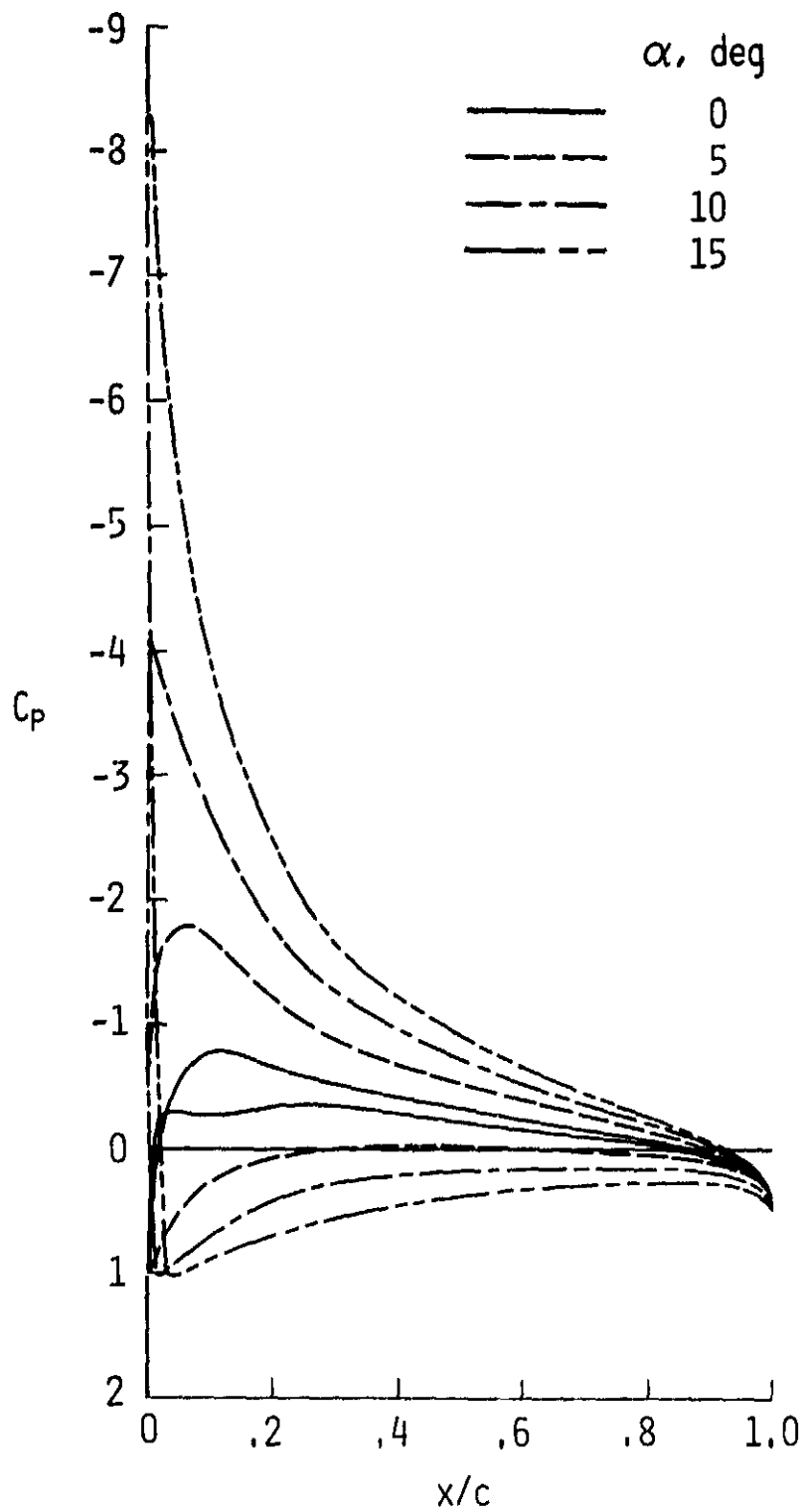
Fig. 14 - Inviscid low speed pressure distri-
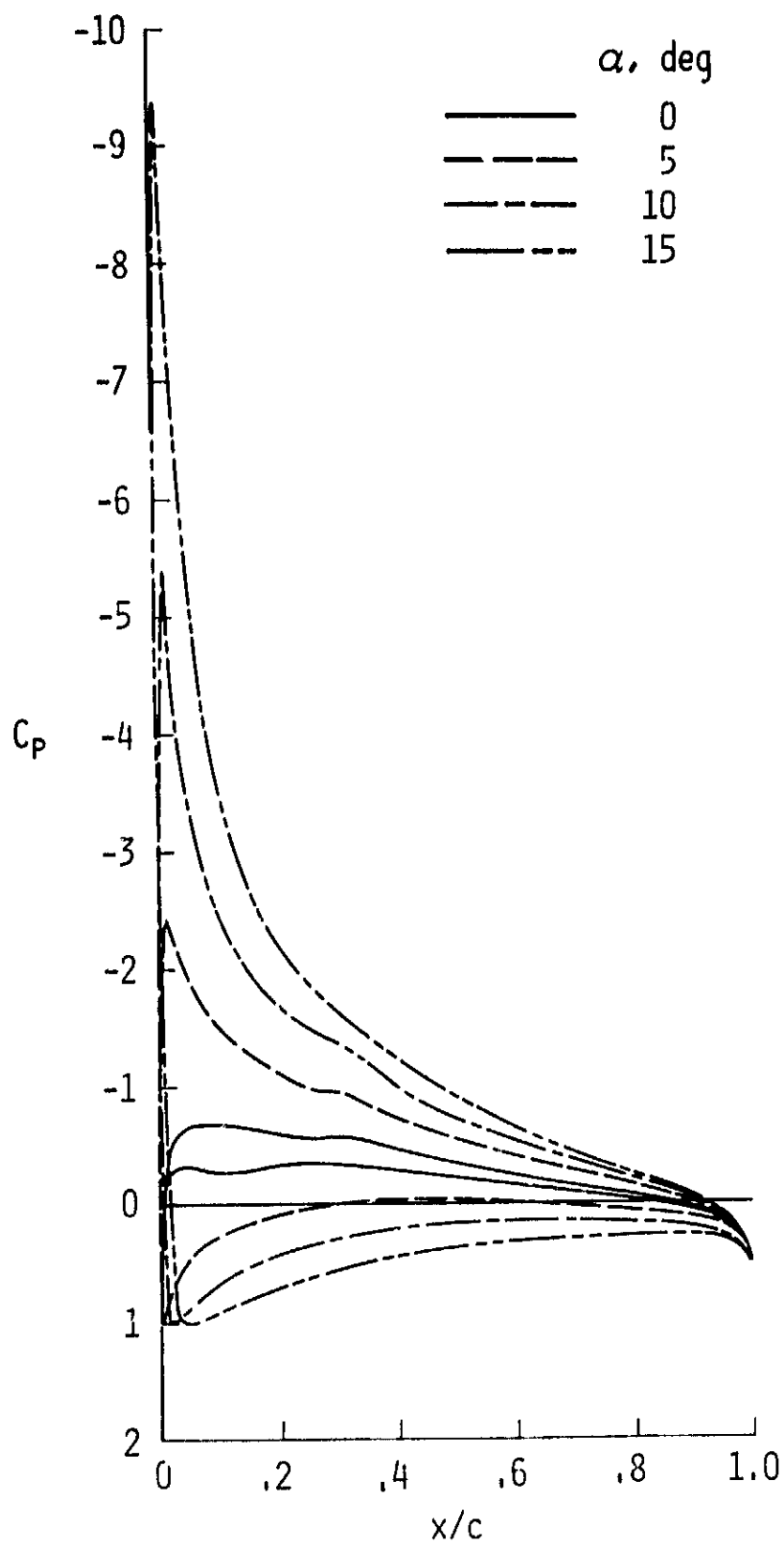butions for NACA 23015 airfoil; M = 0.1

Fig. 15 - Inviscid low speed pressure distri-
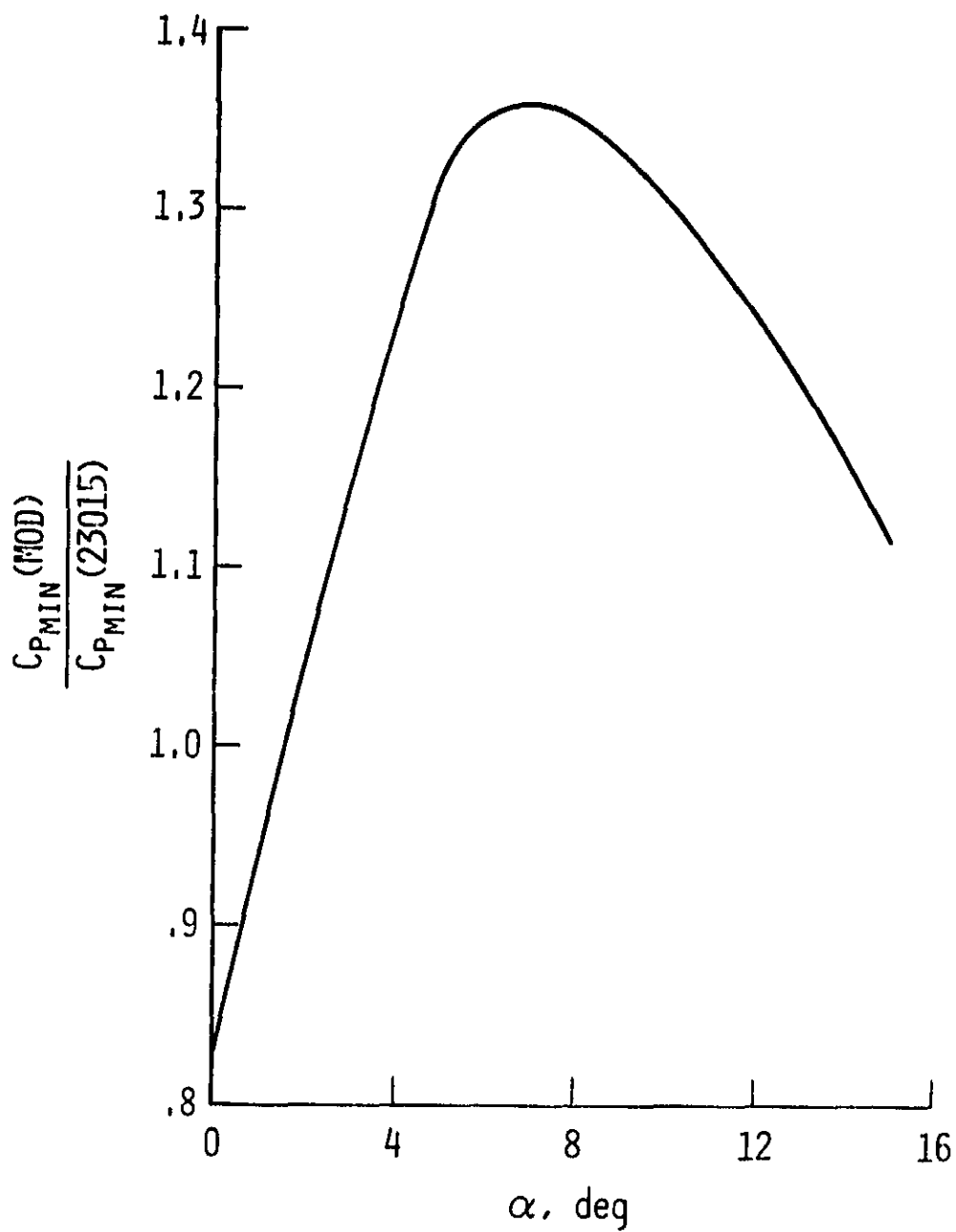butions for the modified NACA 23015 air-
foil; M = 0.1

Fig. 16 – Ratio of $C_{p_{min}}$ for the NACA 23015
airfoil to $C_{p_{min}}$ for the modified 23015
airfoil; M = 0.1

C_P^*

	c_l	c_d	c_m
	0.194	0.0060	-0.0570
	0.215	0.0021	-0.0253

INITIAL AIRFOIL (NACA 64A109)
FINAL AIRFOIL

C_P

x/c

y/c

-1.6
-1.2
-.8
-.4
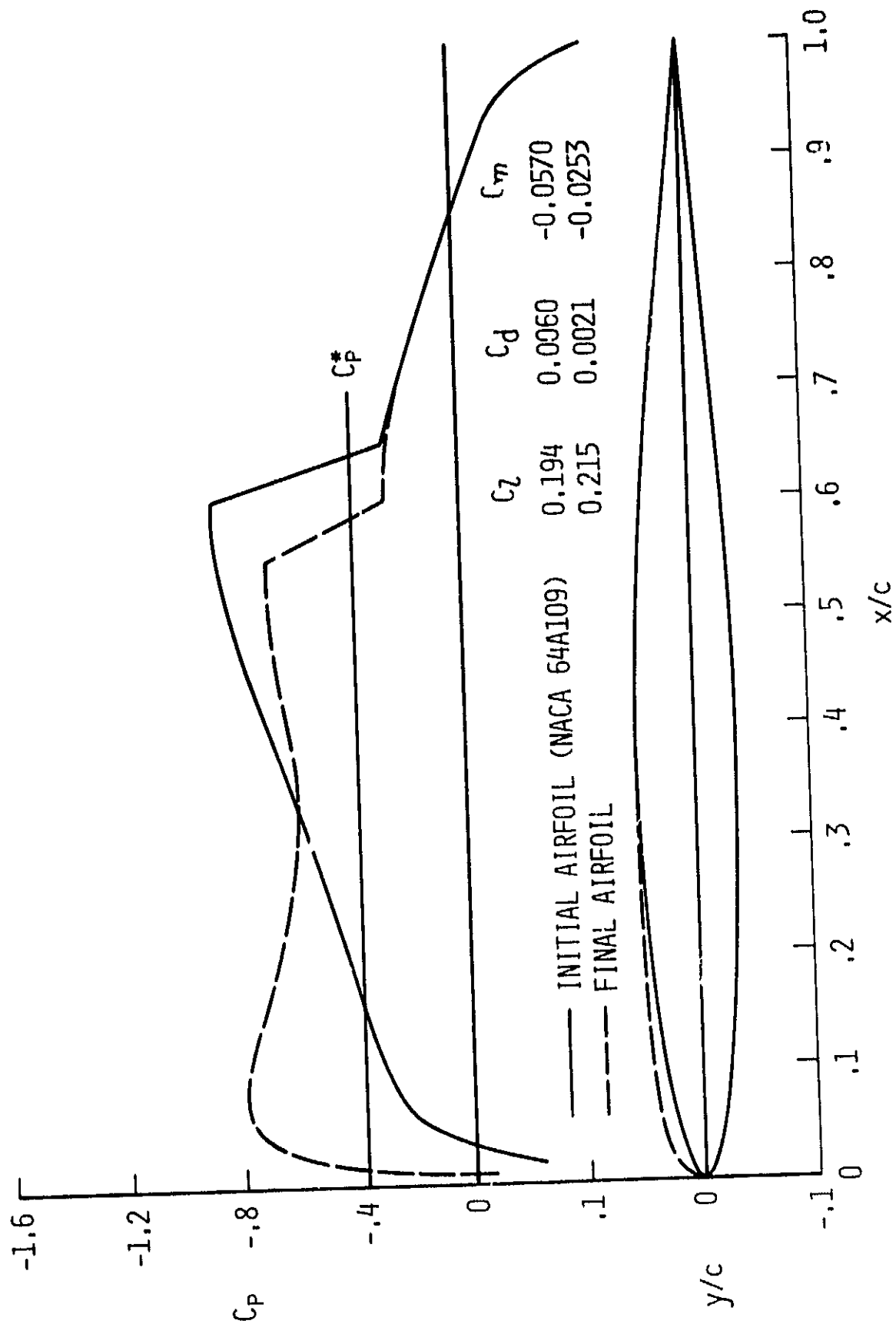0
.1
0
-.1

0   .1   .2   .3   .4   .5   .6   .7   .8   .9   1.0

Fig. 17 - Inviscid drag minimization; M = 0.82, $\alpha = 0°$